

# Grazing-Exit and Micro X-ray Fluorescence Analyses for Chemical Microchips

Kouichi TSUJI,<sup>\*1,\*2†</sup> Tetsuya EMOTO,<sup>\*1</sup> Yosuke NISHIDA,<sup>\*1</sup> Eiichiro TAMAKI,<sup>\*3</sup>  
Yoshikuni KIKUTANI,<sup>\*4</sup> Akihide HIBARA,<sup>\*2,\*3</sup> and Takehiko KITAMORI<sup>\*3,\*4</sup>

<sup>\*1</sup> Department of Applied Chemistry, Graduate School of Engineering, Osaka City University (OCU),  
Sugimoto 3-3-138, Sumiyoshi-ku, Osaka 558-8585, Japan

<sup>\*2</sup> JST-PRESTO, 4-1-8 Honcho Kawaguchi, Saitama 332-0012, Japan

<sup>\*3</sup> Department of Applied Chemistry, School of Engineering, University of Tokyo,  
7-3-1 Hongo, Bunkyo, Tokyo 113-8656, Japan

<sup>\*4</sup> Kanagawa Academy of Science and Technology (KAST), 3-2-1 Sakato, Takatsu, Kawasaki 213-0012, Japan

Grazing-exit x-ray fluorescence (GE-XRF) and micro x-ray fluorescence ( $\mu$ -XRF) methods were applied to chemical microchips as a detection method. Since an energy-dispersive x-ray detector was used, the simultaneous detection of multiple elements was possible. An analyzing region was especially designed on the microchip so that a sample solution could be dried and concentrated in a suitable area corresponding to the size of the primary x-ray beam. Finally, it was confirmed that both analytical methods could be combined well for use with a microchip. In GE-XRF, the background intensity in the XRF spectrum was reduced at grazing-exit angles. In addition, a good relationship between the x-ray fluorescence intensities and the concentrations of standard solutions that were introduced into the microchip was obtained. This indicates that the GE-XRF method is feasible for trace elemental analysis in chemical microchip systems. In  $\mu$ -XRF, an attempt was made to concentrate and dry the analyte within a small analyzing region. The preliminary results indicated that the  $\mu$ -XRF method could be applied for the analysis of microchips.

(Received February 28, 2005; Accepted April 5, 2005)

## Introduction

A chemical microchip has been developed in the semiconductor industry using microfabrication techniques. This microchip is also known as a "micro-TAS (total analysis system)" or "lab-on-a-chip". In chemical microchips, microchannels (diameter, several to several hundred-micrometer) are manufactured on a small substrate of several tens of mm<sup>2</sup>. Various chemical processes, such as mixing, chemical reactions, and separation, are performed on the chemical microchip. Due to the small volume of the channel, chemical processes occur very efficiently. The small size of the chemical microchip is also one of the major advantages when considering *in-situ* analysis in the fields of medical and environmental monitoring.

Usually, visible-UV absorption spectroscopy or laser spectroscopy is used for the final detection of chemical species on a microchip.<sup>1,2</sup> Actually, it is not difficult to combine these nondestructive methods to the analysis of a chemical microchip. Laser spectroscopic methods, such as thermal lens microscopy (TLM), have been successfully used for analyzing very small amounts (1 fL) of analyte in chemical microchips.<sup>3</sup> However, simultaneous multiple element analysis using these methods is usually difficult.

X-ray fluorescence (XRF) analysis also enables nondestructive elemental analysis. When an energy-dispersive

x-ray detector is used in XRF analysis, simultaneous multiple element analysis is possible. Recently, a desktop XRF instrument became commercially available because of the development of small x-ray sources and x-ray detectors. This kind of small XRF instrument is exactly fitted for use with small microchips. Miller *et al.*<sup>4</sup> has applied a micro-XRF method to a capillary electrophoresis (CE) apparatus. They reported simultaneous analysis for Cu and Co using the CE apparatus. Here, improving the sensitivity in XRF analysis is one of the important remaining tasks. The detection limits in XRF have gradually been improved through recent technological advances in x-ray sources, x-ray optics, and x-ray detectors.<sup>5</sup> Special configurations, such as total reflection XRF (TXRF), have also improved the detection limits.<sup>6,7</sup> The TXRF method requires an optically flat substrate over a large area. Therefore, it has been especially applied to the analysis of contamination on silicon wafers. In this article, the grazing-exit XRF method,<sup>8,9</sup> which is as sensitive as TXRF, is applied for the elemental analysis of chemical microchips. As shown in Fig. 1(a), x-ray fluorescence is measured at grazing-exit angles from the surface of the sample. Since the x-ray intensity of the background is reduced under grazing-exit conditions, the detection limits are expected to improve.<sup>8</sup> Compared to TXRF, one of the advantages of GE-XRF is that it enables the analysis of micro-regions.

In another approach, a micro-XRF ( $\mu$ -XRF) technique was investigated for analyzing microchips, as shown in Fig. 1(b). Recently, x-ray microbeams of several tens of micrometer have become available. This x-ray beam diameter almost

<sup>†</sup> To whom correspondence should be addressed.  
E-mail: tsuji@a-chem.eng.osaka-cu.ac.jp

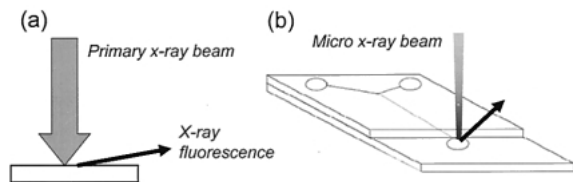


Fig. 1 Experimental ideas for grazing-exit XRF (a) and micro-XRF (b).

corresponds to the size of the channels on microchips. Therefore, application of the  $\mu$ -XRF method to a chemical microchip is reasonable. In this case, there is a possibility of directly monitoring the elemental compositions in the channel. However, we considered that it would be preferable for the purposes of trace analysis to concentrate and dry the analyte. Therefore, we designed a special microchip having a small hollow for  $\mu$ -XRF analysis.

## Experimental

### Microchip for GE-XRF

When GE-XRF is applied, it is important that the sample solution be dried into a homogenous film on a flat substrate. Therefore, we designed a special microchip, as shown in Fig. 2. This microchip has a dendritic microchannel system. Therefore, the sample solution, which is introduced from a hole in the right side, as shown in Fig. 2, is almost automatically pumped due to the capillarity effect. Each channel has a diameter of about 100  $\mu\text{m}$ , and leads to open grating-type multi-channels, where the sample solution is dried in a limited area of  $10 \times 10 \text{ mm}^2$ . As shown at the left side of Fig. 2, the multi-channels have dimensions of 1–5  $\mu\text{m}$  in height and 10  $\mu\text{m}$  in width. The multi-channels are open to air for XRF analysis because the x-ray fluorescence is easily absorbed by the material of the microchip. We expected that the sample solution would be enlarged in the multi-channels due to capillarity.

### Microchip for $\mu$ -XRF

As described later, our  $\mu$ -XRF instrument is equipped with a polycapillary x-ray lens, which consists of more than several million capillaries. This x-ray lens enables us to obtain an x-ray microbeam with a diameter of 50  $\mu\text{m}$ .<sup>10</sup> This diameter corresponds to the diameter of the channel; it is about 100  $\mu\text{m}$  in the microchip. Therefore, a direct analysis by  $\mu$ -XRF of the solution in the channel is reasonable. However, the absorption of x-rays by the solution is a serious problem. After the sample solution is dried, an analysis of the residue is required for trace elemental analysis by XRF. Thus, we attempted to concentrate the analyte in a small hollow region (400  $\mu\text{m}$  in diameter), which is shown in Fig. 3. The sample solution in the channel was trapped in the hollow and dried by local heating. To concentrate the sample efficiently, small polystyrene beads (10  $\mu\text{m}$  in diameter) were packed in the hollow. The concentrated samples in the hollow were measured by  $\mu$ -XRF.

### GE-XRF instrument

Figure 4 shows the experimental setup for the GE-XRF measurement. A sealed-type x-ray tube (Mo target) was used at a voltage of 30 kV and a current of 20 mA. The primary x-rays were guided with a tube (diameter: about 10 mm) onto the microchip at a right angle. X-ray fluorescence emitted from the

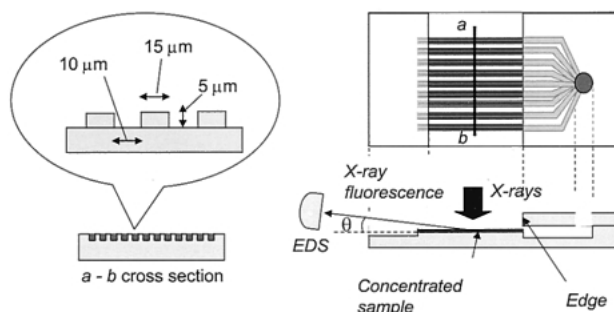


Fig. 2 Drawing of a microchip designed for GE-XRF analysis.

sample was measured by an energy-dispersive x-ray detector (silicon drift detector (SDD), X Flash detector-type 1201, Rontec, Germany). This detector has a sensitive area of 10  $\text{mm}^2$  and an energy resolution of < 150 eV at Mn  $K_{\alpha}$ . To change the exit angle ( $\theta$  in Fig. 2), the detector was placed on a single-axis movement stage, which was driven by a stepper motor with a minimum step of 1  $\mu\text{m}$  and controlled by a computer. A slit (width: 100  $\mu\text{m}$ ) was perpendicularly attached at the top of the detector at a distance of 77 mm from the sample to obtain good angular resolution. Under these measurement conditions, an angular resolution of 0.07 degrees was obtained.

### Micro-XRF instrument

Figure 5 shows the experimental setup for  $\mu$ -XRF measurement.<sup>10</sup> X-rays emitted from the Mo target of the x-ray tube were input to a polycapillary lens made at the X-Ray Optics Laboratory of the Normal Beijing University. An x-ray spot size of approximately 50  $\mu\text{m}$  was obtained at an output focal distance of 15 mm from the end of the lens. The microchip, shown in Fig. 3, was placed at the exact focal point. X-ray fluorescence was detected by the SDD at a distance of 30 mm from the sample and at a take-off angle of about 40 degrees.

### Sample and microchip preparation

A standard sample solution of Fe was prepared at a concentration of 1.033 mg/ml. This sample solution was inserted in the channel of the microchip by using a microsyringe pump with a speed of 0.2 ml/h. Introduction of the solution was observed by an optical microscope.

Both microchips were manufactured at the University of Tokyo. The surface of each microchip was treated with an acid solution, alcohol, and a NaOH solution to produce hydrophilicity. The edge (shown in Fig. 2) between the dendritic channels and the opened multi-channels was treated with octadecyltrimethoxysilane to produce hydrophobicity. After these surface treatments, the sample solution moved smoothly into the multi-channels, where the solution was dried in air at room temperature.

## Results and Discussion

### Applications of GE-XRF

It was confirmed that the sample solution could be smoothly introduced and enlarged on the grating channels region by treating the surface of the microchip to produce hydrophilicity. The problem of sample preparation that remained was that some portion of the solution stayed at the edge between the microchannels and the multi-channels, although the edge was

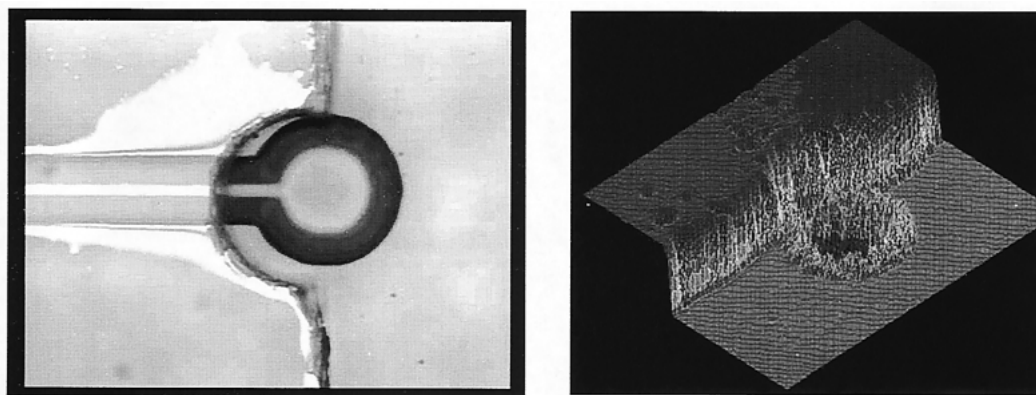


Fig. 3 Small hollow produced at end of a channel on a microchip for  $\mu$ -XRF analysis. Optical microscope image (left) and 3-D image of the hollow (right).

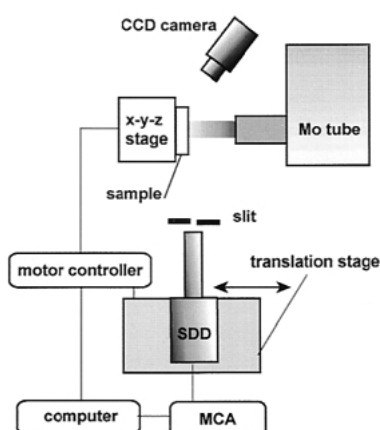


Fig. 4 Experimental setup for GE-XRF analysis.

treated to be hydrophobic. Therefore, it was difficult to concentrate the entire sample in the multi-channels. This problem will be resolved by improving the microchip design and the surface-treatment procedure.

The sample solution of the Fe standard solution was introduced into the microchip, as shown in Fig. 2, and dried in air. After the solution was dried, the residue was measured by GE-XRF. Figures 6(a) and (b) show the x-ray spectra measured at the two exit angles of 40 and 0.5 degrees, respectively. In both spectra, the characteristic peaks of Fe appeared. However, continuous x-rays near the peak were strongly observed when XRF was measured at the large exit angle of 40 degrees, as shown in Fig. 6(a). Under the grazing-exit conditions, the detection of x-rays emitted from deep inside was reduced, while x-ray fluorescence from the near surface was emphasized. Consequently, the continuous x-ray intensity was decreased.

GE-XRF is usually applied for optically flat substrates. In this work, a special sample carrier having a grating structure was used. Since the x-ray measurement was performed in the direction of the grooves, the surface can be considered to be *quasi* flat for a GE-XRF measurement. Therefore, surface sensitive analysis would be possible with a low background level, as shown in Fig. 6(b).

Standard solutions of Fe and Cu of different concentrations were introduced into the microchip. First, x-ray fluorescence was measured as a function of the exit angle. Figure 7 shows the dependence of the Fe  $K_{\alpha}$  intensity on the exit angle, as

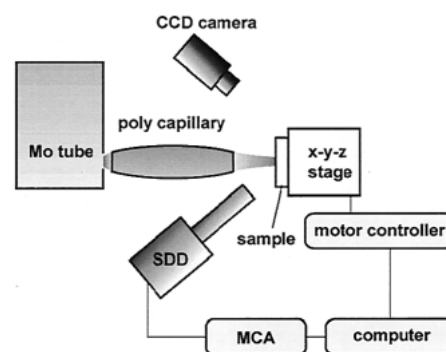


Fig. 5 Experimental setup for  $\mu$ -XRF analysis.

measured for the standard solution (500 ppm). The x-ray fluorescence intensity was normalized at the maximum. To change the exit angle, the SDD, shown in Fig. 4, was moved. This movement is plotted in Fig. 7. The x-ray fluorescence increased as the exit angle increased. In the x-axis range of more than 1700  $\mu\text{m}$  in Fig. 7, the intensity decreased because the slit on the SDD obstructed the x-ray fluorescence. Next, the x-ray spectrum was recorded with a counting time of 300 s at the fixed SDD position where the x-ray intensity showed 50% of maximum. Figure 8 shows the relationship between the x-ray fluorescence intensities (Cu  $K_{\alpha}$  and Fe  $K_{\alpha}$ ) and the concentrations of the standard solutions. Good agreements were obtained with correlation coefficients of 0.994 and 0.991 for Cu and Fe, respectively. This result suggests the possibility of semi-quantitative analysis of microchips by GE-XRF.

#### Applications of $\mu$ -XRF

We investigated how the sample solution could be concentrated in the hollow. However, it was difficult to concentrate the sample in only the hollow because the sample solution easily overflowed from it before drying. Therefore, we investigated the possibility of achieving a more effective concentration by using polystyrene beads and other special polymers in the hollow. This paper shows the experimental results obtained with the use of the polystyrene beads. A mixed solution of  $\text{CuSO}_4$  (1.09 g/L, 17.3 mM) and  $\text{CdCl}_2$  (1.94 g/L, 17.3 mM) was introduced into the microchip. The total input volume was 23.8 nL, which included 25.9 ng Cu and 46.1 ng Cd. The mapping results obtained for Cu, S, Cd, and Cl are shown in Fig. 9. Every element was nearly observed

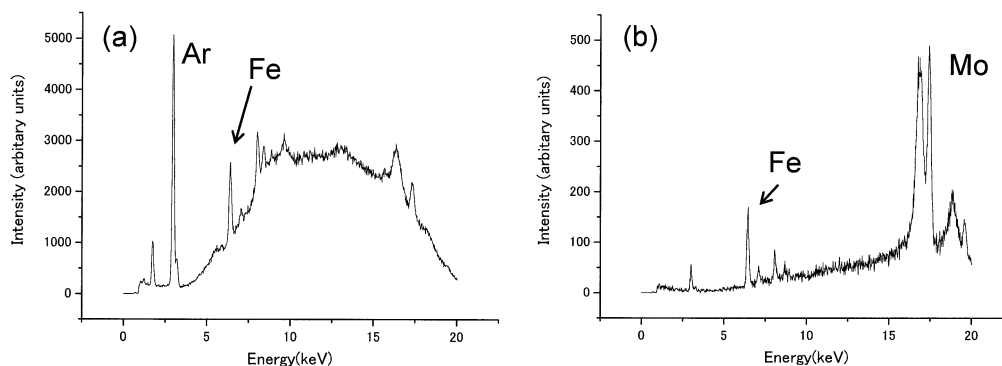


Fig. 6 X-ray spectra measured by  $\mu$ -XRF instrument at different exit angles of 40 degrees (a) and 0.5 degrees (b).

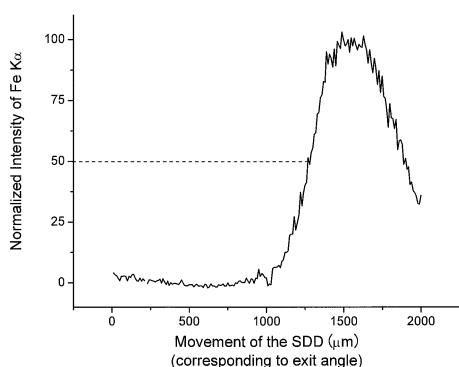


Fig. 7 Exit-angle dependence of the normalized intensity of Fe  $K_{\alpha}$ . The standard solution (500 ppm) was introduced into the microchip. The x-axis indicates the movement of the SDD shown in Fig. 4, which corresponds to the variation of the exit angle.

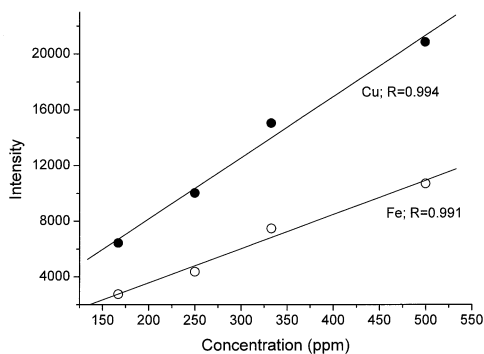


Fig. 8 Relationship between the x-ray fluorescence intensities (Cu  $K_{\alpha}$  and Fe  $K_{\alpha}$ ) and concentration of standard solutions that were introduced into the microchip.

homogeneously at one location. Some of the polystyrene beads overflowed from the hollow due to the movement of the solution. However, it was confirmed that the analyte was present and concentrated on the polystyrene beads. This suggests that concentrating the analyte on polystyrene beads is effective.

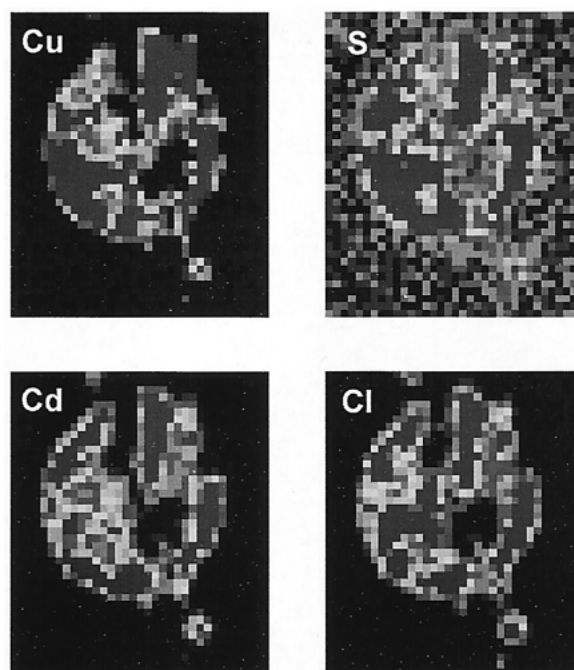


Fig. 9 X-ray elemental maps of Cu, Cd, S, and Cl, measured at the hollow on the microchip.

## Conclusions

The x-ray fluorescence methods of GE-XRF and  $\mu$ -XRF were applied to chemical microchips, which were newly designed for this purpose. Preliminary results showed that these XRF methods would be feasible in the detection of an analyte in the microchip. In GE-XRF, a good relationship between the x-ray fluorescence intensities (Cu  $K_{\alpha}$  and Fe  $K_{\alpha}$ ) and the concentrations of standard solutions that were introduced into the microchip was obtained with correlation coefficients of 0.994 and 0.991 for Cu and Fe, respectively. These results suggest the possibility for the semi-quantitative analysis of microchips by GE-XRF. However, further improvement of the microchips, themselves, will be necessary. The x-ray spectra observed by GE-XRF had a considerably large background intensity, suggesting that the grazing-exit condition was not actually realized. The grating type multi-channels were effective for collecting the sample solutions. However, they produced large

scattered x-rays, leading to a large background intensity. A simple microchip having a flat area for GE-XRF analysis is currently being designed. Treating the surface so that it is hydrophilic will expand the region of analysis of the introduced solution. We believe that the  $\mu$ -XRF method is suitable as a final detection method for chemical microchips. Actually, the preliminary results shown in Fig. 9 suggest the possibility for concentrating the sample solution in a small region for analysis. However, further precise control of the movement and drying of the solutions is required for quantitative analysis.

### Acknowledgements

Financial support for this work was provided by Japan Society for the Promotion of Science (JSPS) Grants-in-Aid (B-15350048 and 15656176) and by the JST-PRESTO project.

### References

1. Z. Liang, N. Chiem, G. Ocvirk, T. Tang, K. Fluri, and D. J. Harrison, *Anal. Chem.*, **1996**, *68*, 1040.
  2. M. L. Chabinyk, D. T. Chiu, J. C. McDonald, A. D. Stroock, J. F. Christian, A. M. Karger, and G. M. Whitesides, *Anal. Chem.*, **2001**, *73*, 4499.
  3. T. Kitamori, M. Tokeshi, A. Hibara, and K. Sato, *Anal. Chem.*, **2004**, *76*, 53A.
  4. T. C. Miller, M. R. Joseph, G. J. Havrilla, C. Lewis, and V. Majid, *Anal. Chem.*, **2003**, *75*, 2048.
  5. K. Tsuji, J. Injuk, and R. E. Van Grieken (ed.), "X-Ray Spectrometry: Recent Technological Advances", **2004**, John Wiley & Sons, Ltd.
  6. Y. Yoneda and T. Horiuchi, *Rev. Sci. Instrum.*, **1971**, *42*, 1069.
  7. R. Klockenkamper, "Total Reflection X-ray Fluorescence", **1997**, John Wiley & Sons, Ltd.
  8. K. Tsuji, "Grazing-Exit X-Ray Spectrometry", in "X-Ray Spectrometry: Recent Technological Advances", ed. K. Tsuji, J. Injuk, and R. E. Van Grieken, **2004**, John Wiley & Sons, Ltd., 293.
  9. K. Tsuji, K. Wagatsuma, K. Hirokawa, T. Yamada, and T. Utaka, *Spectrochim. Acta B*, **1997**, *52*, 841.
  10. T. Emoto, Y. Sato, Y. Konishi, X. Ding, and K. Tsuji, *Spectrochim. Acta B*, **2004**, *59*, 1291.
-